Applied Catalysis B: Environmental 89 (2009) 597–601

Contents lists available at ScienceDirect

Applied Catalysis B: Environmental

journal homepage: www.elsevier.com/locate/apcatb

Synthesis of sulfated ZrO_2/MWCNT composites as new supports of Pt catalysts for direct methanol fuel cell application

Dao-Jun Guo [a,b], Xin-Ping Qiu [a,*], Wen-Tao Zhu [a], Li-Quan Chen [a]

[a] Key Laboratory of Organic Optoelectronics and Molecular Engineering, Department of Chemistry, Tsinghua University, Beijing 100084, China
[b] School of Chemistry and Chemical Engineering, Qufu Normal University, Qufu, Shandong 273165, PR China

ARTICLE INFO

Article history:
Received 13 November 2008
Received in revised form 22 January 2009
Accepted 27 January 2009
Available online 3 February 2009

Keywords:
Electrocatalyst
Solid superacid
Methanol oxidation
Proton conductivity
Direct methanol fuel cell

ABSTRACT

Sulfated zirconia supported on multi-walled carbon nanotubes as new supports of Pt catalyst (Pt–S-ZrO_2/MWCNT) was synthesized with aims to enhance electron and proton conductivity and also catalytic activity of Pt electrocatalyst in terms of larger concentrations of ionizable OH groups on surfaces. Fourier transform infrared spectroscopy analysis shows that the sample surfaces were modified with sulfate. Transmission electron microscopy results show that the Pt and sulfated ZrO_2 particles dispersed relatively uniformly on the surface of the multi-walled carbon nanotube. X-ray diffraction shows that S-ZrO_2 and Pt coexist in the Pt–S-ZrO_2/MWCNT composites and S-ZrO_2 has no effect on the crystalline lattice of Pt. Pt–S-ZrO_2/MWCNT catalyst was evaluated in terms of the electrochemical activity for methanol electro-oxidation using cyclic voltammetry, steady-state polarization experiments and electrochemical impedance spectroscopy technique at room temperature. Pt–S-ZrO_2/MWCNT catalyst show higher catalytic activity for methanol electro-oxidation compared with Pt catalyst on non-sulfated ZrO_2/MWCNT support and commercial Pt/C (E-TEK).

1. Introduction

The problem of the poor performance of the methanol fuel cells is a problem of poor catalyst performance. It is well known that when pure platinum is used as the catalyst, it will be rapidly poisoned by the adsorption of CO produced during the oxidation of methanol. However, many investigations have shown that some Pt-based alloy or Pt-metal oxide catalysts exhibit enhanced tolerance of CO and, consequently, improved electrocatalytic activities compared to those with platinum alone [1–5]. For instance, two mechanisms have been proposed to account for the promotional effect of Pt–Ru alloy catalysts. One is the so-called bifunctional mechanism [6–8] in which the role of ruthenium is to dissociate water to form adsorbed OH species, which then reacts with adsorbed CO to generate CO_2. Another explanation is the electronic ligand effect mechanism, i.e. the electronic properties of platinum are modified by Pt–Ru orbital overlaps so that the binding strength of CO adsorbed on Pt is weakened, leading to the enhancement of electrocatalytic activities for methanol electro-oxidation [9,10]. Unfortunately, the Ru element is also very expensive, which restricts the wide application of PtRu-based catalysts in direct alcohol fuel cells (DAFCs). Thus high cost of DAFCs can be solved by a transition from noble metal to new inexpensive materials.

Recently, another strategy by using some other metal oxides such as CeO_2, ZrO_2, TiO_2 and so on modified (or coated) carbon black (CB) or carbon nanotube (CNT) as the support of Pt catalysts have also been developed, in which the metal oxides can also enhance the CO tolerance of the catalysts according to the bifunctional mechanism [11–15]. The results reported in the literature confirm that these fillers are indeed effective in improving the catalytic activity of Pt catalyst. In general, there are three types of Pt species exit in the Pt/metal oxide/CNTs catalyst, as shown in Scheme 1a. (I) Pt deposits on the surface of CNTs, which is the same as pristine Pt/CNTs catalyst. (II) Pt deposits on the interface of CNTs and metal oxide, which causes the most active interface site of the catalyst, when Pt contact well with CNTs and metal oxide. According to the bifunctional mechanism, the OH_{ads} species on metal oxide can transform CO-like poisoning species (CO_{ads}) on Pt to CO_2, releasing the active sites on Pt for further electrochemical reaction. (III) Pt deposits on the surface of metal oxides, which may be useless due to the bad electron conductivity of metal oxide. To solve this problem and increase the utilization of Pt catalysts, alternative materials with high electron and proton conductivity are strongly aspired for.

Mixed proton-electron conducting materials should be ideal catalyst supports for direct methanol fuel cells (DMFCs) since they allow for low ohmic resistance in both the proton and electron

* Corresponding author. Tel.: +86 10 62794234; fax: +86 10 62794234.
E-mail address: qiuxp@mail.tsinghua.edu.cn (X.-P. Qiu).

0926-3373/$ – see front matter © 2009 Published by Elsevier B.V.
doi:10.1016/j.apcatb.2009.01.025

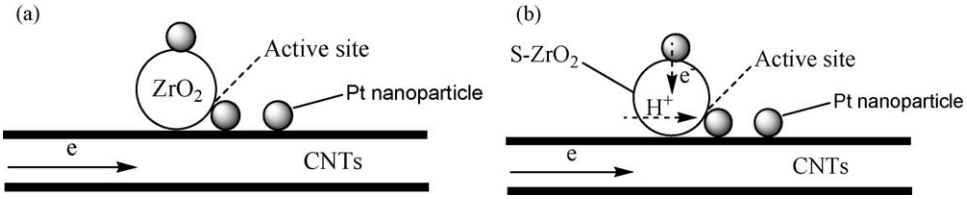

Scheme 1. Schematic diagrams of the novel catalysts.

conduction at the same time, which can result in a much more catalytic active catalyst for methanol oxidation. Sulfated ZrO_2, known as SO_4^{2-}–ZrO_2 solid superacid, is proton conductor with high conductivity because of the SO_4^{2-} group on ZrO_2 surface can increase the hydrophilic properties of ZrO_2 [16,17]. On the other hand, it is easier to form smaller nanoparticles and result in higher surface area compared with non-modified ZrO_2 [16]. A composite catalyst combining the sulfated ZrO_2 nanoparticles in contact with Pt catalysts and multi-walled carbon nanotube (MWCNT) support we described here takes into account high electron and proton conductivity. In summary, sulfated ZrO_2/MWCNT composites have several advantages: (1) doping of this nanocrystalline ZrO_2 with sulfuric acid yielded a high-surface-area superacid and the presence of the H_2SO_4 did not change textural properties. So Pt nanoparticles supported on sulfated ZrO_2 should have a higher surface area and the Pt utilization can be increased. (2) It is well known that the oxidation of CO requires an adsorbed OH species adjacent to the adsorbed CO. The SO_4^{2-} group on ZrO_2 surface will increase the hydrophilic properties of ZrO_2 and the more dissociative hydroxyl of H_2O absorbed on the solid superacid than that non-sulfated ZrO_2, thus sulfated ZrO_2 can more easily transform CO_{ads} to CO_2 by the hydroxyl on its surface according to the bifunctional mechanism, releasing the active sites of Pt for further electrochemical reaction. (3) Sulfated ZrO_2 is superacid and good proton conductor, as support for Pt catalyst may increase the utilization of the Pt catalyst for methanol oxidation because of the proton conductivity shown as in Scheme 1b. The obtained catalysts with 20 wt% Pt loading on the support and a Pt:S-ZrO_2 ratio of 1:2 shows superb performance for direct electro-oxidation of methanol.

2. Experimental

2.1. Synthesis of S-ZrO_2/MWCNT supported Pt (Pt–S-ZrO_2/MWCNT) electrocatalyst

For preparing S-ZrO_2/MWCNT composites, multi-walled carbon nanotubes, zirconium oxychloride hydrate ($ZrOCl_2{\cdot}8H_2O$), ammonia (NH_3) and sulfuric acid (H_2SO_4) were used as the starting material, precipitating agent and sulfating agent, respectively. Twenty-eight percent NH_3 aq. was gradually dropped into $ZrOCl_2{\cdot}8H_2O$ solution (0.20 M) with appropriate amounts of MWCNTs and the mixture was adjusted to pH 10, the mixture was stirred for 24 h. Then the obtained $ZrO_2{\cdot}nH_2O$ sol was washed with distilled water using centrifuge till chloride ions were not detected by silver nitrate ($AgNO_3$), dried at 110 °C for 10 h and ground. The $ZrO_2{\cdot}nH_2O$ and MWCNT composites were added to 0.50 M H_2SO_4 with vigorously stirring for 15 min, then were filtrated and dried at 90 °C. After that, the powder was calcinated at 550 °C under N_2 flow for 1 h, the S-ZrO_2/MWCNT supports thus prepared is denoted as S-ZrO_2/MWCNTs. For comparison, the ZrO_2/MWCNT composites were also obtained with the same process without H_2SO_4 added.

Afterwards, S-ZrO_2/MWCNT powder and appropriate amounts of $H_2PtCl_6{\cdot}6H_2O$ were dispersed in 50 mL Millipore water to prepare a suspended solution. A freshly prepared solution of $NaBH_4$ was added dropwise into the above solution under vigorous stirring. After 30 min, the product is collected by centrifugation, washed several times with H_2O and ethanol, the obtained catalyst was dried in a vacuum oven at 70 °C overnight, then the 20 wt% Pt loading on the support and a Pt:S-ZrO_2 ratio of 1:2 catalysts was obtained denoted as Pt–S-ZrO_2/MWCNT. For comparison, Pt-ZrO_2/MWCNT composites with the same contents of Pt and ZrO_2 nanoparticles were also obtained directly by reducing the Pt precursor in ZrO_2/MWCNT suspension using the addition of $NaBH_4$ at room temperature.

2.2. Measurement

Electrochemical reactivity of the catalysts was measured by cyclic voltammetry (CV) using a three-electrode cell at the PARSTAT 2273 potentiostat controlled by PowerSuite® software (Princeton Applied Research). The working electrode was a gold plate covered with a thin layer of Nafion-impregnated catalyst. As a typical process, the catalyst ink was prepared by ultrasonically dispersed about 1 mg catalyst in the 25 μL mixture of Nafion solution (20% Nafion and 80% ethylene glycol) for 30 min. After casting the catalysts ink onto a polished planar gold patch (1.0 cm × 1.0 cm), the electrodes were air-dried at 80 °C for 1 h. Pt gauze and a saturated calomel electrode (SCE) were used as counter electrode and reference electrode, respectively. All potentials in this report are quoted versus SCE. CV test was conducted at 50 mV s^{-1} in a solution of 1 M $HClO_4$ with 1 M CH_3OH, potential ranging from −0.2 to 1.0 V. The electrochemical impedance spectroscopy (EIS) measurements of the samples were performed at a potential of 0.5 V vs. SCE in the frequency range of 100 kHz and 0.1 Hz. All the electrochemical measurements were conducted under 25 °C.

The morphology of Pt–S-ZrO_2/MWCNT composites were investigated using high-resolution transmission electron microscopy (HRTEM, JEOL model JEM-2100) operated at 200 kV. The XRD

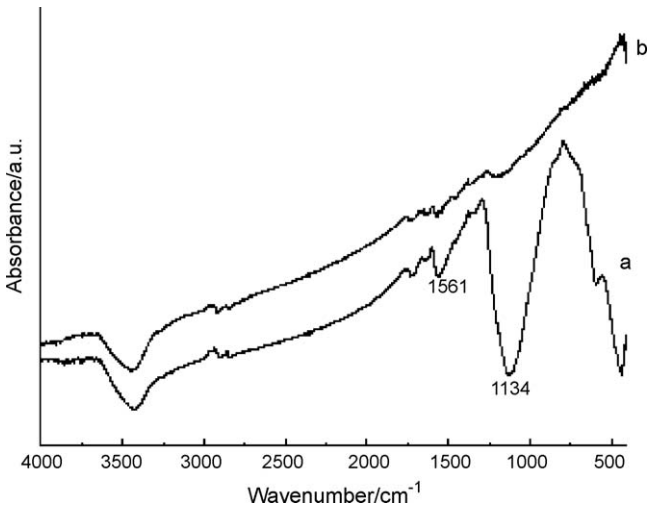

Fig. 1. IR spectroscopy of S-ZrO_2/MWCNT (a) and ZrO_2/MWCNT (b) composites.

patterns of the as-prepared products were investigated via a Bruker powder diffraction system (model D8 Advanced), using Cu K_α as the radiation source at the operating voltage of 40 kV and a scan rate of 6° min^{-1}. The FT-IR spectra were recorded in the range of 4000–400 cm^{-1} on a Spectrometer (GX FT-IR, PerkinElmer, CA, USA), equipped with a DTGS detector. Each spectrum was an average of accumulation of 32 scans at a resolution of 4 cm^{-1}.

3. Results and discussion

3.1. IR spectra analysis of the S-ZrO_2/MWCNT composites

Infrared spectra of S-ZrO_2/MWCNT composite are illustrated in Fig. 1. For comparison, a spectrum of ZrO_2/MWCNT before H_2SO_4 was added is also presented. As was expected, a large difference was confirmed between S-ZrO_2/MWCNT and ZrO_2/MWCNT composites. In Fig. 1a, the intense broad peaks between 800 and 1300 cm^{-1} assigned to the S=O bond or S–O bond are the characteristic peaks. But for S-ZrO_2/MWCNT samples in this work, because S-ZrO_2 is nanoparticle, the fine structure splitting of IR spectra disappear, only a broad band between 1300 and 800 cm^{-1} showed attributing to the sulfated vibrational modes. This implies the presence of high-concentration SO_x bonded tightly with Zr, which leads to a high proton conductivity [18,19]. The weak peak at 1561 cm^{-1} is assigned to the dissociative hydroxyl of H_2O absorbed on the solid superacid. Thus sulfated ZrO_2 can more easily transform CO_{ads} on Pt nanoparticle to CO_2 by the hydroxyl on its surface according to the bifunctional mechanism [20].

3.2. TEM analysis of the Pt–S-ZrO_2/MWCNT composites

Fig. 2 shows the typical TEM and HRTEM images of the Pt–S-ZrO_2/MWCNT composites. It can be seen that the Pt and S-ZrO_2 nanoparticles are relatively uniformly distributed on the sidewalls of the MWCNTs. The diameter of the Pt or S-ZrO_2 particles is about only 3–8 nm, and has a mean value at 5 nm. The nanoparticles layer coating on the MWCNT surfaces can also be identified in the image and the thickness of nanoparticle layer is about 8 nm. Thus, two-dimensional Pt–S-ZrO_2/MWCNT composites were obtained by using MWCNT as carrier materials. The HRTEM micrograph reveals further that both Pt and S-ZrO_2 nanoparticles attached on the sidewalls of the MWCNTs, the presence of Pt and S-ZrO_2 nanoparticles can be further confirmed in the XRD results. It can also be seen that there are at least three cases for Pt nanoparticles location on MWCNT surface. The first case is that some Pt catalysts are deposited on MWCNT surface with no contact with S-ZrO_2. The second case is that some Pt nanoparticles have contacts closely with S-ZrO_2. The last case is that some Pt nanoparticles are deposited on the surface S-ZrO_2. Because of excellent proton conductivity of sulfated ZrO_2, these Pt catalysis supported on S-ZrO_2 can also be used for methanol electro-oxidation.

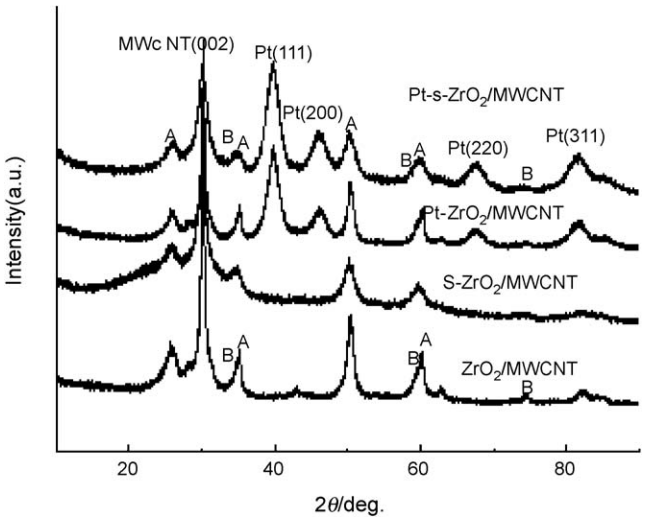

Fig. 3. XRD analysis of Pt–S-ZrO_2/MWCNT, Pt-ZrO_2/MWCNT, S-ZrO_2/MWCNT and ZrO_2/MWCNT composites.

3.3. XRD analysis of the Pt–S-ZrO_2/MWCNT composites

Fig. 3 shows the XRD patterns of Pt–S-ZrO_2/MWCNT and S-ZrO_2/MWCNT compared with that of Pt-ZrO_2/MWCNT and ZrO_2/MWCNT. For both the patterns of Pt–S-ZrO_2/MWCNT and Pt-ZrO_2/MWCNT, the diffraction peaks of Pt, S-ZrO_2 and ZrO_2 can be observed indicating their coexistence in the sample. The characteristic peaks of face centered cubic crystalline platinum at about 39°, 46°, 68° and 81°, are corresponding to Pt (1 1 1), (2 0 0), (2 2 0) and (3 1 1) plane, respectively. And there is no shift in any of the diffraction peaks of platinum in Pt–S-ZrO_2/MWCNT and Pt–ZrO_2/MWCNT catalyst indicating that the addition of S-ZrO_2 and ZrO_2

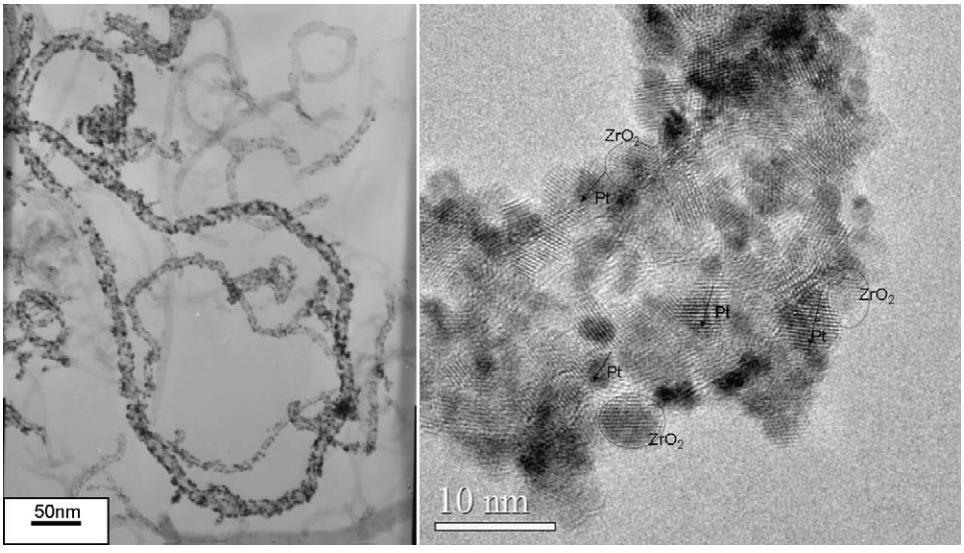

Fig. 2. TEM and HRTEM images of Pt–S-ZrO_2/MWCNT composites.

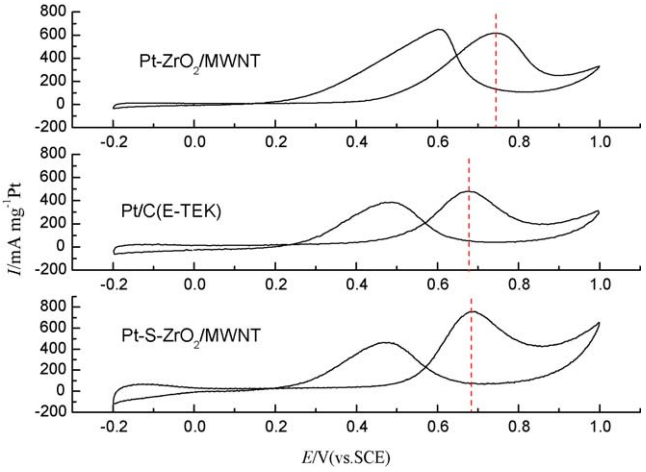

Fig. 4. Cyclic voltammograms of various electrodes at 50 mV s^{-1} in 1.0 M $HClO_4$ + 1.0 M CH_3OH aqueous solution.

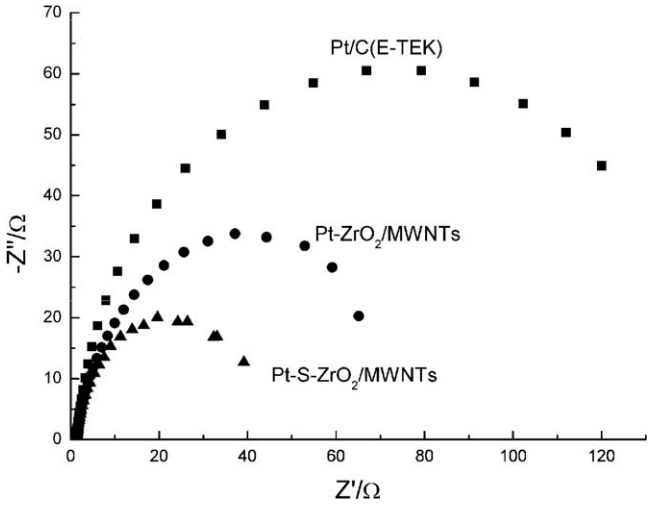

Fig. 6. Nyquist plots of EIS for methanol electro-oxidation on Pt–S-ZrO_2/MWCNT, Pt-ZrO_2/MWCNT and Pt/C electrode in 1.0 M $HClO_4$ + 1.0 M CH_3OH solution at 0.5 V.

has no effect on the crystalline lattice of platinum. On the other hand, X-ray diffraction data for two samples of S-ZrO_2/MWCNT and ZrO_2/MWCNT indicated both the tetragonal (B) and monoclinic (A) phase of ZrO_2 form. The breadth of the XRD peaks also indicated that small Pt and S-ZrO_2 crystallites were obtained. The average crystal size of Pt and S-ZrO_2 nanoparticles estimated using Scherrer equation was about 4.2 and 7.8 nm, respectively, which is confirmed by TEM micrographs.

3.4. Electrochemical properties of Pt–S-ZrO_2/MWCNT composites

The Pt–S-ZrO_2/MWCNT samples were tested for their catalytic activity in the electro-oxidation of methanol. To investigate the role played by the sulfated ZrO_2 coating further, Pt-ZrO_2/MWCNT catalyst with the same Pt and commercial Pt/C (E-TEK; 20 wt% on Vulcan) were prepared for comparison. Fig. 4 shows voltammetric curves recorded for the synthesized and reference catalysts in 1 M CH_3OH and 1 M $HClO_4$ as supporting electrolyte. The peak currents due to methanol oxidation in the forward scan for Pt–S-ZrO_2/MWCNT, Pt–ZrO_2/MWCNT and the E-TEK Pt/C catalyst are 752.7, 621.4 and 481.9 mA mg^{-1} Pt, respectively. Pt–S-ZrO_2/MWCNT displays 1.6 times higher current density than the Pt/C catalyst and 1.2 times than Pt–ZrO_2/MWCNT catalyst. Pt–S-ZrO_2/MWCNT appears to be significantly more active for methanol oxidation. Furthermore, the peak potential of Pt–S-ZrO_2/MWCNT is lower than that of Pt–ZrO_2/MWCNT and very similar to that of Pt/C, indicating that Pt–S-ZrO_2/MWCNT composites showed sufficient both electron and proton conductivity, which caused no large iR loss in the methanol oxidation.

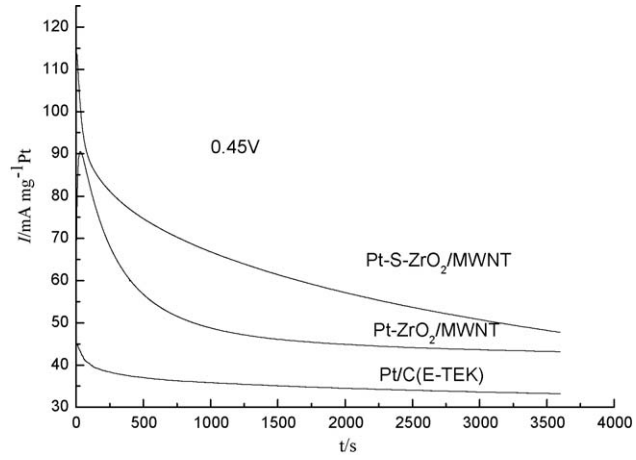

Fig. 5. Chronoamperograms of various electrodes at 0.45 V in 1.0 M $HClO_4$ + 1.0 M CH_3OH aqueous solution.

Fig. 5 shows that the pattern of current decay was different for each catalyst. For both the catalysts, the current decayed continuously even after 1 h, supposedly because of catalyst poisoning by the chemisorbed carbonaceous species and the depletion of OH sites which are responsible for oxidation of CO [21,22]. The Pt–S-ZrO_2/MWCNT was able to maintain the highest current density throughout all the ranges up to 3600 s among all the catalysts. The catalytic activity of Pt–S-ZrO_2/MWCNT catalysts was much higher than that of Pt–ZrO_2/MWCNT and Pt/C, this would be due to the strengthening of both the bifunctional mechanism and higher electron and proton conductivity of S-ZrO_2/MWCNT composites, as is consistent with the CV results.

All the above results of CV and chronoamperometry tests indicate that Pt–S-ZrO_2/MWCNT exhibits higher catalytic activity for methanol oxidation than Pt-ZrO_2/MWCNT and commercial Pt/C. This can be confirmed further from the results of the electrochemical impedance spectroscopy measurements that were carried out on Pt–S-ZrO_2/MWCNT, Pt-ZrO_2/MWCNT and Pt/C at a potential of 0.5 V vs. SCE, and the corresponding Nyquist plots are shown in Fig. 6. In the spectra, the diameter of arc is a measure of charge transfer resistance (R_{ct}) related to the charge transfer reaction kinetics during the methanol oxidation process on the Pt–S-ZrO_2/MWCNT and Pt-ZrO_2/MWCNT catalysts. Examination of Fig. 6 shows a significant decrease of R_{ct} for Pt–S-ZrO_2/MWCNT, indicating a decrease in reaction resistance. A significant decrease of R_{ct} values for Pt–S-ZrO_2/MWCNT indicates a smaller reaction resistance and higher catalytic activity for methanol oxidation in acid solution on Pt–S-ZrO_2/MWCNT electrode.

4. Conclusions

S-ZrO_2/MWCNT supported Pt catalyst was synthesized in the present work. FT-IR analysis revealed that SO_x exists on the surface of S-ZrO_2 particles. Pt was dispersed on the S-ZrO_2/MWCNT composite surface with a diameter of 4.2 nm. The Pt–S-ZrO_2/MWCNT composites exhibited higher methanol electro-oxidation activity than Pt-ZrO_2/MWCNT and commercial Pt/C. The charge transfer resistance of Pt–S-ZrO_2/MWCNT is also smaller than that of Pt-ZrO_2/MWCNT as found in the impedance spectra, indicating an increase in reaction kinetics. The application of sulfated metal oxides, such as S-ZrO_2 as co-catalyst of Pt appears to be a promising

and less expensive methanol oxidation anode catalyst. Efforts are fostered in tailoring the present catalyst system and understanding surface site interactions.

Acknowledgement

China Postdoctoral Science Foundation funded project (Project No. 20070410075, 200801068).

References

[1] H.A. Gasteiger, N. Markovic, P.N. Ross, E.J. Cairns, J. Phys. Chem. 98 (1994) 617–625.
[2] A. Kabbabi, R. Faure, R. Durand, B. Beden, F. Hahn, J.M. Leger, C. Lamy, J. Electroanal. Chem. 444 (1998) 41–53.
[3] A. Hamnett, Catal. Today 38 (1997) 445–457.
[4] D.R. Rolison, P.L. Hagans, K.E. Swider, J.W. Long, Langmuir 15 (1999) 774–779.
[5] J.W. Long, R.M. Stroud, K.E. Swider-Lyons, D.R. Rolison, J. Phys. Chem. B 104 (2000) 9772–9776.
[6] T. Frelink, W. Visscher, J.A.R. van Veen, Langmuir 12 (1996) 3702–3708.
[7] H.A. Gasteiger, N. Markovic, P.N. Ross, E.J. Cairns, J. Electrochem. Soc. 141 (1994) 1795–1803.
[8] H.N. Dinh, X.M. Ren, F.H. Garzon, P. Zelenay, S. Gottesfeld, J. Electroanal. Chem. 491 (2000) 222–233.
[9] H.F. Oetjen, V.M. Schmidt, U. Stimming, F. Trila, J. Electrochem. Soc. 143 (1996) 3838–3842.
[10] J.B. Goodenough, A. Hamnett, B.J. Kennedy, R. Manoharan, S.A. Weeks, J. Electroanal. Chem. 240 (1988) 133–145.
[11] H.Q. Song, X.P. Qiu, F.H. Li, Electrochim. Acta 53 (2008) 3708–3713.
[12] H.J. Kim, D.Y. Kim, H. Han, Y.G. Shui, J. Power Sources 159 (2006) 484–490.
[13] Y.X. Bai, J.J. Wu, J.Y. Xi, J.S. Wang, W.T. Zhu, L.Q. Chen, X.P. Qiu, Electrochem. Commun. 7 (2005) 1087–1090.
[14] M. Takahashi, T. Mori, F. Ye, A. Vinu, J. Am. Ceram. Soc. 90 (2007) 1291–1294.
[15] J.S. Wang, J.Y. Xi, Y.X. Bai, Y. Shen, J. Sun, L.Q. Chen, W.T. Zhu, X.P. Qiu, J. Power Sources 164 (2007) 555–560.
[16] Z.M. Wu, G.Q. Sun, W. Jin, H.Y. Hou, S.L. Wang, Q. Xin, J. Membr. Sci. 313 (2008) 336–343.
[17] Y. Suzuki, A. Ishihara, S. Mitsushima, N. Kamiya, K.-I. Ota, Electrochem. Solid-State Lett. 10 (2007) B105–B107.
[18] G. Colon, M.C. Hidalgo, G. Munuera, I. Ferino, M.G. Cutrufello, J.A. Navio, Appl. Catal. B: Environ. 63 (2006) 45–59.
[19] S. Hara, M. Miyayama, Solid State Ionics 168 (2004) 111–116.
[20] Y.X. Bai, J.J. Wu, X.P. Qiu, J.Y. Xi, J.S. Wang, J.F. g Li, W.T. Zhu, L.Q. Chen, Appl. Catal. B: Environ. 73 (2007) 144–149.
[21] M.A. Scibioh, S.K. Kim, E.A. Cho, T.H. Lim, S.A. Hong, H.Y. Ha, Appl. Catal. B: Environ. 84 (2008) 773–782.
[22] F.H.B. Lima, E.R. Gonzalez, Appl. Catal. B: Environ. 79 (2008) 341–346.